HOMEWORK REPORT

AE305 - NUMERICAL METHODS

AEROSPACE ENGINEERING DEPARTMENT

# Homework #3

# Team #8

*Authors:*
Arda Özuzun (Id:2172765 )
Muhammed Kürşat Yurt (Id:2172971 )
Yusuf Uzuntaş (Id:1882364 )

Date: February 6, 2021

# 1 Introduction

In this homework, flow around a cylinder with radius 1 and NACA0020 airfoil are solved by using finite volume method. Flow is assumed irrotational, inviscid and incompressible which is known as potential flow in literature. Flow fields calculated by solving Laplace's equation for the potential function $\phi$. Velocity vectors of flow is founded by using following equation:

$$\nabla\phi = \vec{V} = u\vec{i} + v\vec{j} \tag{1}$$

General form of Laplace's equation shown below:

$$\frac{\partial \phi}{\partial t} = \frac{\partial^2 \phi}{\partial x^2} + \frac{\partial^2 \phi}{\partial y^2} \tag{2}$$

For steady flow time derivative goes to zero and the governing equation become:

$$\nabla^2\phi = \frac{\partial^2 \phi}{\partial x^2} + \frac{\partial^2 \phi}{\partial y^2} = 0 \tag{3}$$

Where the diffusion coefficient is assumed to be unity. The integral form of the differential equation given below where $\vec{F} = \nabla\phi$

$$\frac{\partial}{\partial t}\int_{\Omega} \phi d\Omega + \oint_{S} \vec{F} \cdot d\vec{S} \tag{4}$$

The boundary conditions for this flow are on the solid surfaces and at the far field boundary are shown below:

$$\nabla\phi_\infty = \vec{V_\infty} \cdot (\cos(\alpha)\vec{i} + \sin(\alpha)\vec{j}) \tag{5}$$

$$\vec{F} \cdot d\vec{S} = 0 \tag{6}$$

# 2 Method

## 2.1 Finite Volume Method

Partial differential equation is represented and evaluated by using finite volume method. In this method, values are calculated at discrete places on a meshed geometry. Volume integrals in a partial differential equation that contain a divergence term are converted to surface integrals using the divergence theorem for the finite volume method.Then fluxes at the surface of each finite volume are evaluated. The general form of finite volume method is:

$$\frac{\partial}{\partial t}(\phi \cdot \Omega) + \sum_{n=1}^{3} \vec{F_n} \cdot \vec{S_n} = 0 \tag{7}$$

## 2.2 Bernoulli Equation

The relationship between velocity and pressure for the inviscid, incompressible flow can be found by the Bernoulli equation. It states that an increase in the velocity of the fluid leads decrease in pressure.

$$p + \frac{1}{2}\rho V^2 = constant \tag{8}$$

Also by the help of the Bernoulli equation form of the pressure coefficient is modified as below:

$$C_p = \frac{p - p_\infty}{q_\infty} \tag{9}$$

$$C_p = 1 - \frac{V^2}{V_\infty^2} \tag{10}$$

## 2.3 Force Coeffecient Calculation Method

$c_l$ is coefficient of lift force and $c_d$ is coefficient of drag force. $c_l$ and $c_d$ are obtained through $c_a$ and $c_n$ where is coefficient of axial and normal force. To obtain $c_a$ and $c_n$ values following formula is used in this homework.

$$c_n = \frac{1}{c}[\int_0^c (c_{p,l} - c_{p,u})dx + \int_0^c (c_{f,u}\frac{dy_u}{dx} + c_{f,l}\frac{dy_l}{dx})dx] \tag{11}$$

$$c_a = \frac{1}{c}[\int_0^c (c_{p,u}\frac{dy_u}{dx} - c_{p,l}\frac{dy_l}{dx})dx + \int_0^c (c_{f,u} + c_{f,l})dx] \tag{12}$$

The fluid is steady,incompressible and inviscid so there is no friction coefficients. Thus the $c_a$ and $c_d$ equation is:

$$c_n = \frac{1}{c}[\int_0^c (c_{p,l} - c_{p,u})dx] \tag{13}$$

$$c_a = \frac{1}{c}[\int_0^c (c_{p,u}\frac{dy_u}{dx} - c_{p,l}\frac{dy_l}{dx})dx] \tag{14}$$

The lift and drag coefficients is founded by using following equation:

$$c_l = c_n cos(\alpha) - c_a sin(\alpha) \tag{15}$$

$$c_d = c_n sin(\alpha) + c_a cos(\alpha) \tag{16}$$

# 3 Results and Discussion

## 3.1 Circle

### 3.1.1 Mesh of Circle

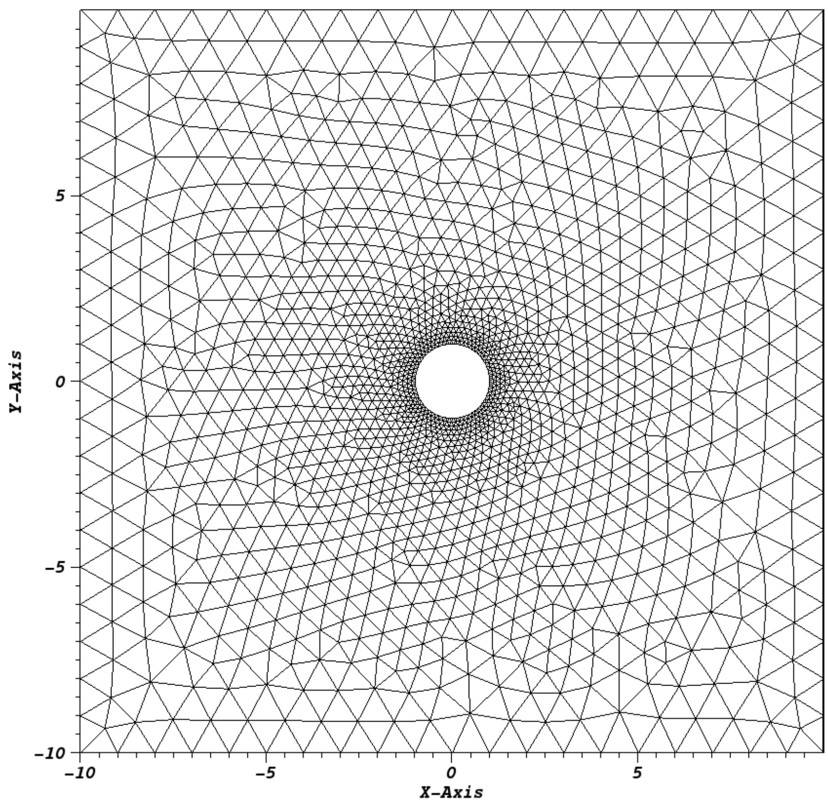


Figure 1: Mesh of Solution Domain of Circle

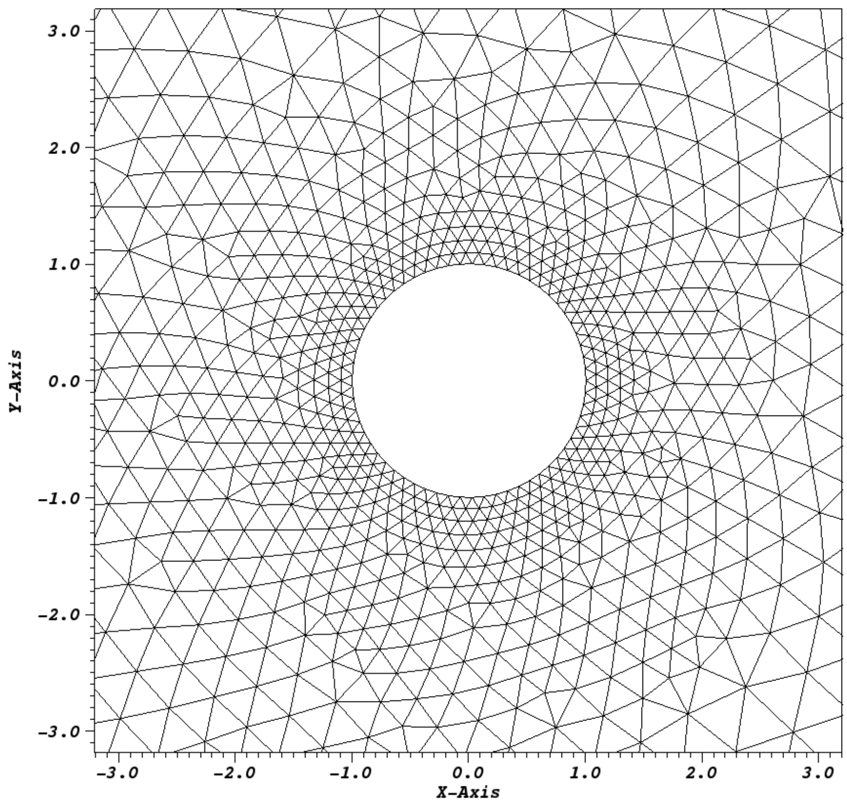


Figure 2: Close Look of Mesh Around Circle

In the Figure 1 and 2 mesh is shown which is between circle and boundary and it is made by using EasyMesh program. The type of the mesh is polygon and in the shape of triangle. On the edge of boundary there are 20 triangle which means its edge size is 1. In order to mesh this circle and its boundary, data file which contains coordinate of circle and boundary is used in the program.

### 3.1.2 Angle of Attack 0

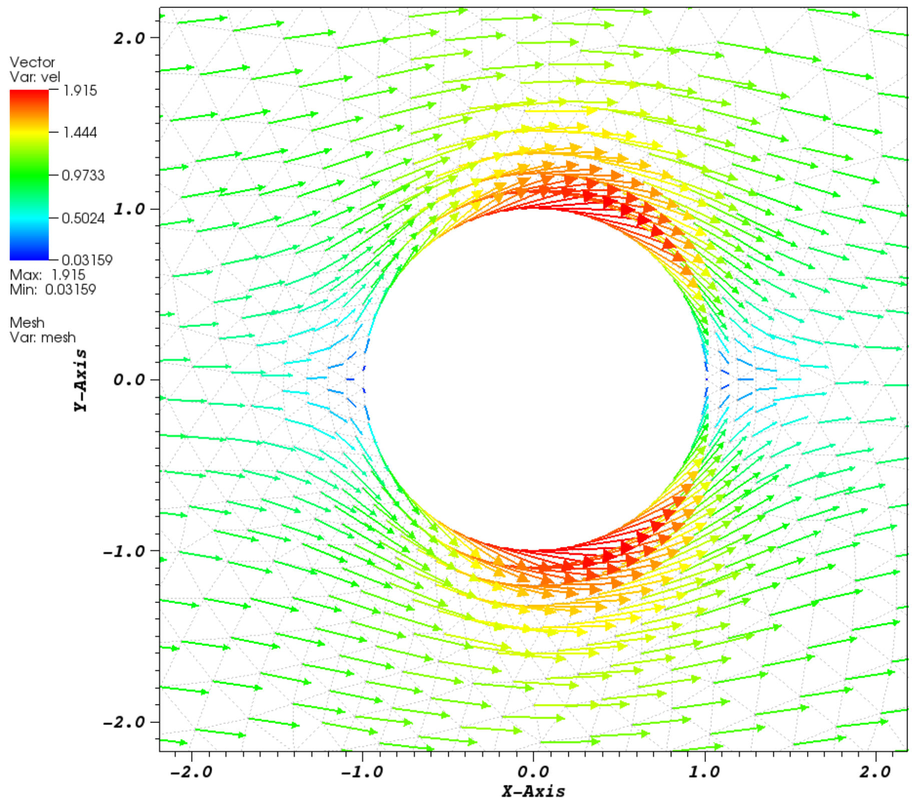


Figure 3: Velocity Vectors Around Circle at Angle of Attack 0

In the Figure 3, velocity fields are shown for the angle of attack is equal zero. It is obvious that velocity is zero at the points where circular body and x axis cross. These points are called stagnation points where velocity is equal to zero.Also it is seen that, velocity maximum at the top and the bottom of the circle. It can be seen that velocity of the fluid, far enough from the circular solid is getting closer to the free stream velocity.

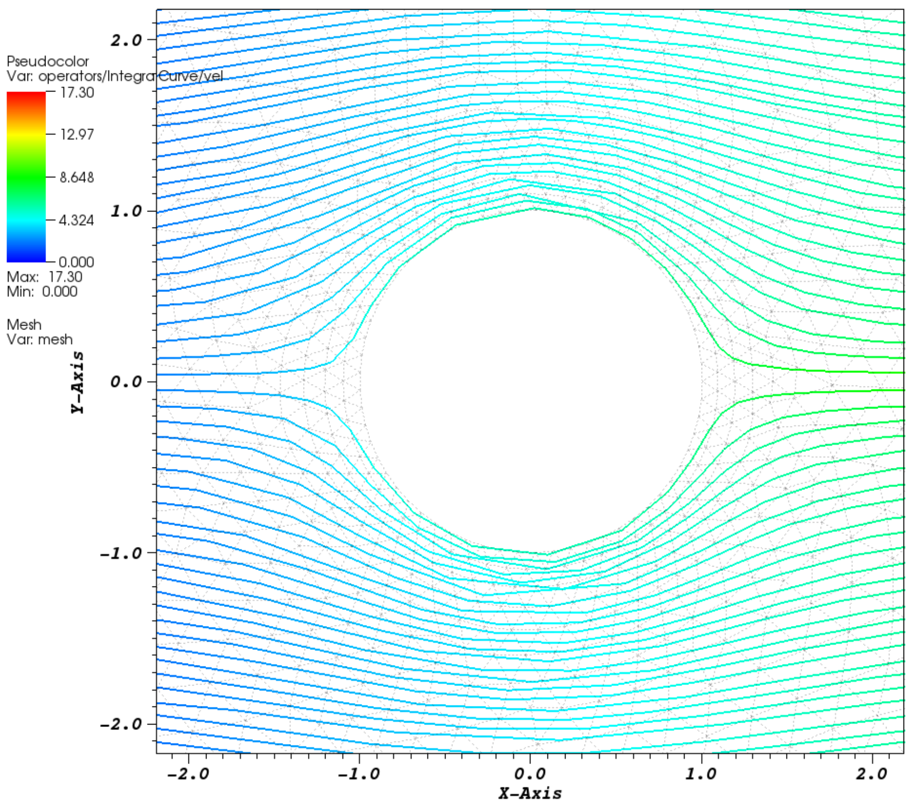


Figure 4: Stream Lines Around Circle at Angle of Attack 0

It can be observed from Figure 4,the streamlines are symmetric for x and y axis. Also, the solid surface itself is a streamline.

### 3.1.3 Angle of Attack 10

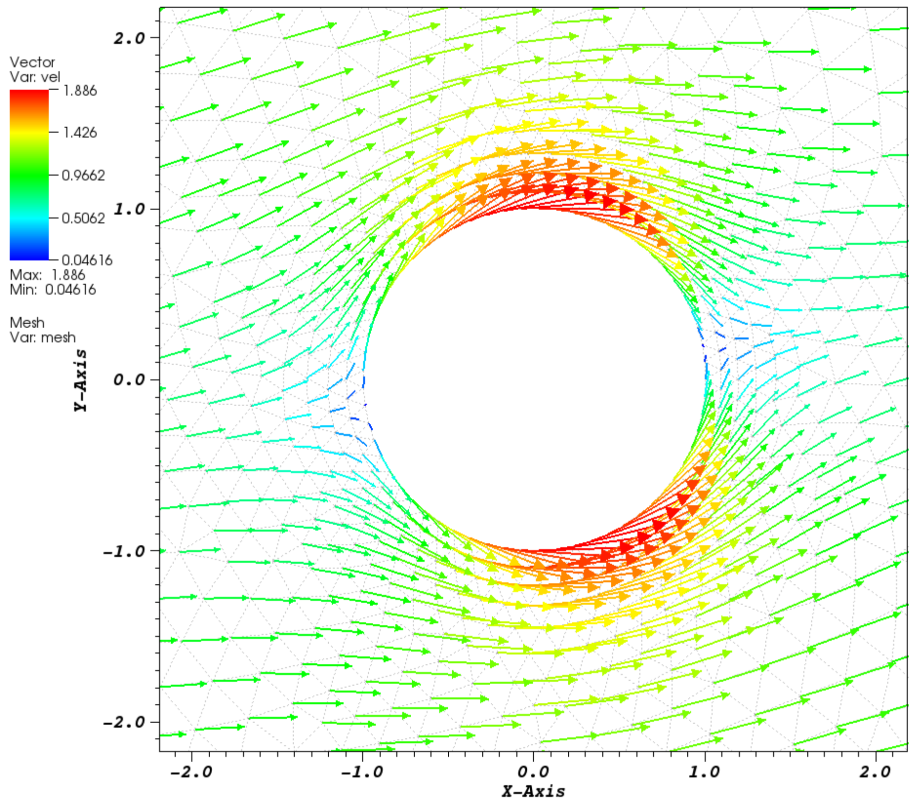


Figure 5: Velocity Vectors Around Cylinder at Angle of Attack 10

It can be seen from figure 5 that at the angle of attack 10 degree, the points where velocity is zero is at the line which pass from the origin and rotated around 10 degree counterclockwise about x axis. It can be observed that thanks to symmetry of circle when angle of attack is changed the solution is just rotated.

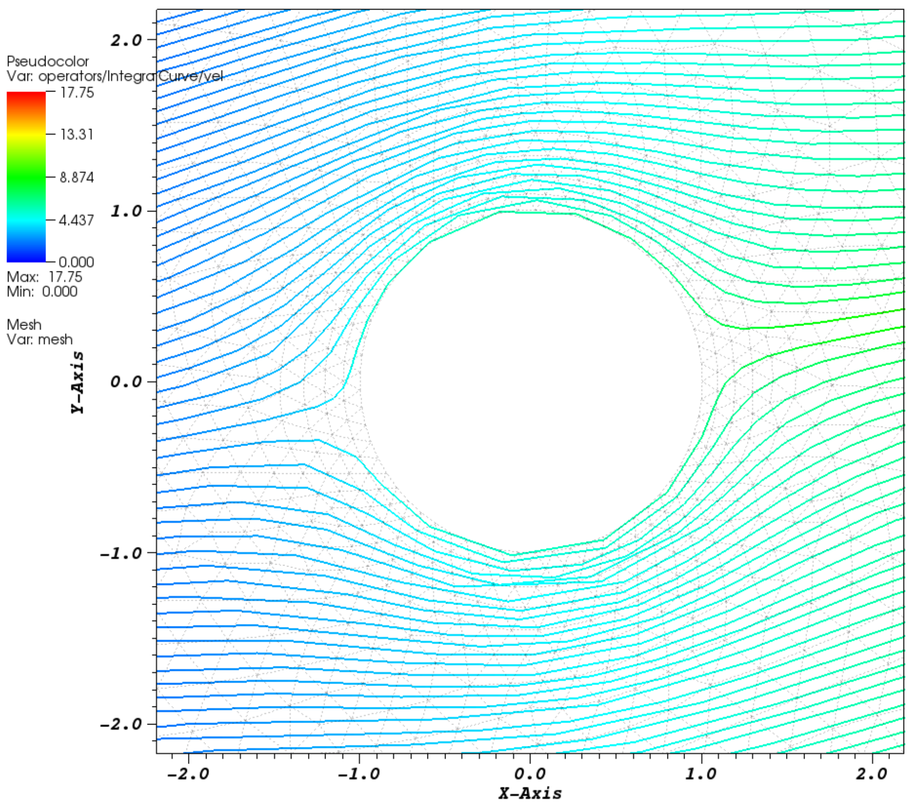


Figure 6: Stream Lines Around Cylinder at Angle of Attack 10

It can be observed from figure 6, the streamlines are almost symmetric for the line which pass the origin and rotated around 10 degree counterclockwise about x axis. Streamlines are also symmetric to the line perpendicular to first one. In addition, the solid surface itself is a streamline.

#### 3.1.4 Comparison of $C_p$ of Cylinder with Theory

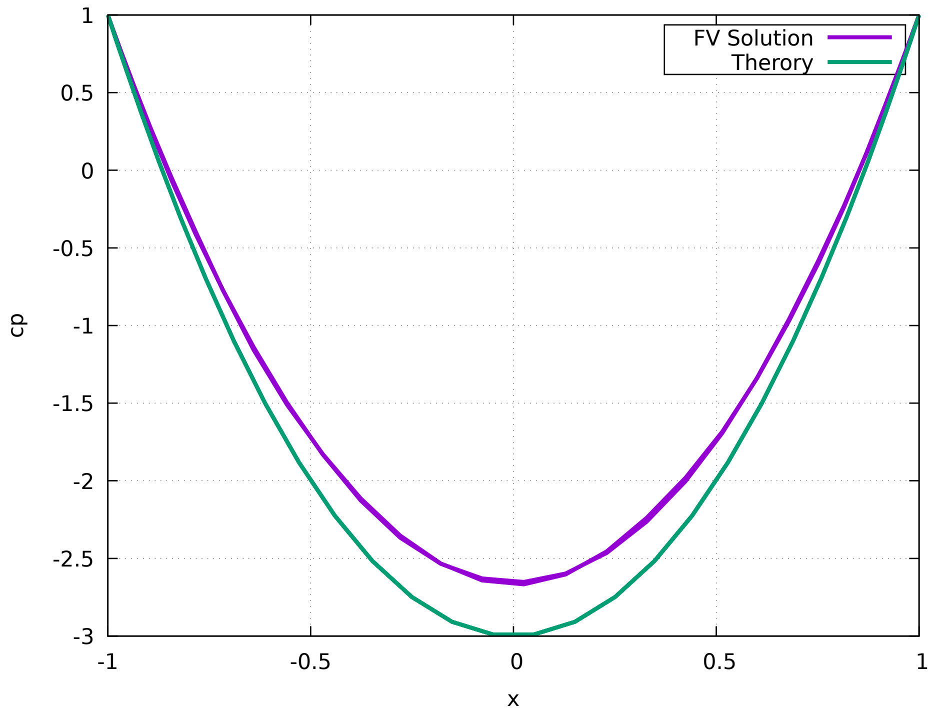


Figure 7: $C_p$ distribution of Cylinder Theoretical versus Numerical

From figure 7 it can be said that there is a difference between numerical and theoretical $C_p$ distribution. This difference is occurs due to the used mesh approach of solution method to solve problem. Since not velocities are actually calculated for cells and then converted for to node point by averaging there would always exist such a difference between numerical solution of FVM and theoretical solution.

## 3.2 Airfoil

### 3.2.1 Mesh of Airfoil

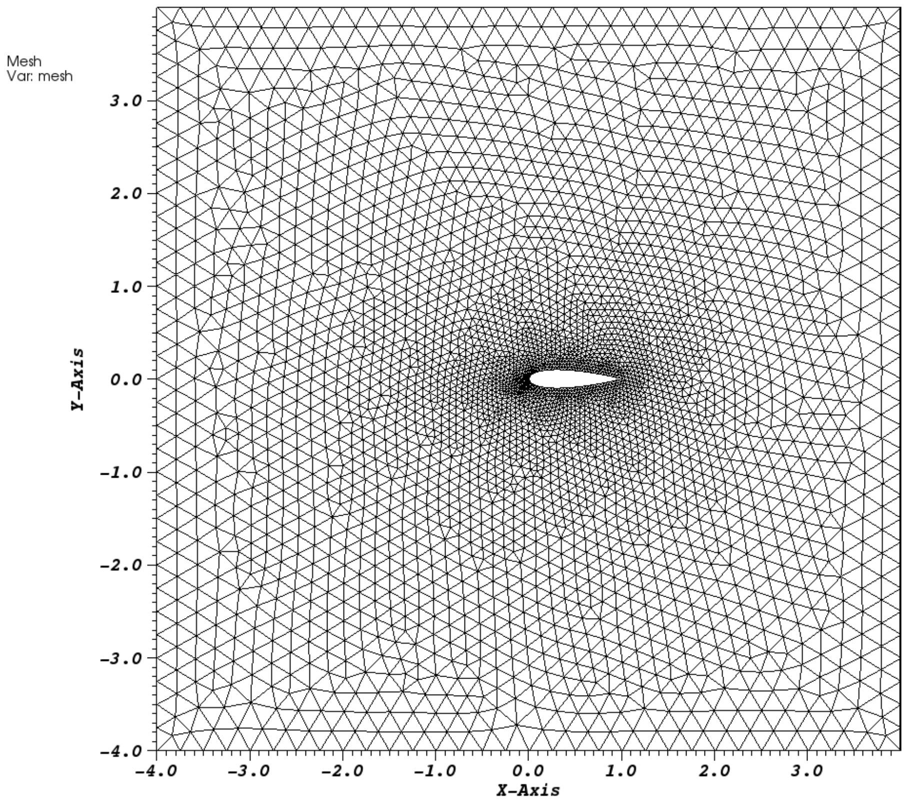


Figure 8: General Solution Domain of Airfoil

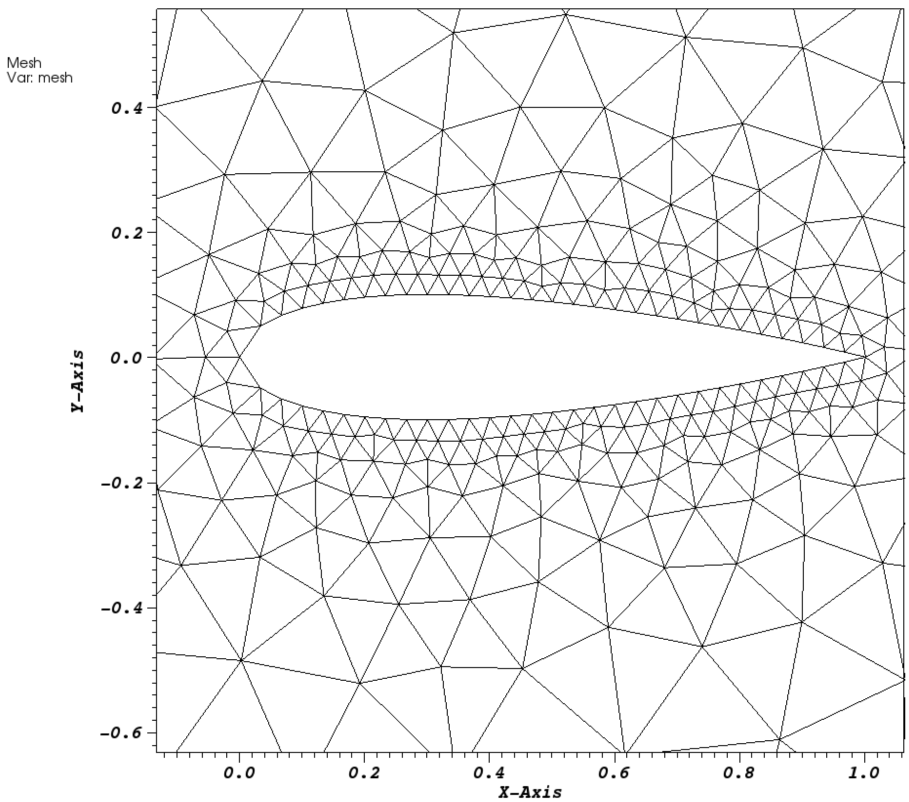


Figure 9: Close Look of Mesh Around Airfoil Using Linear Spacing

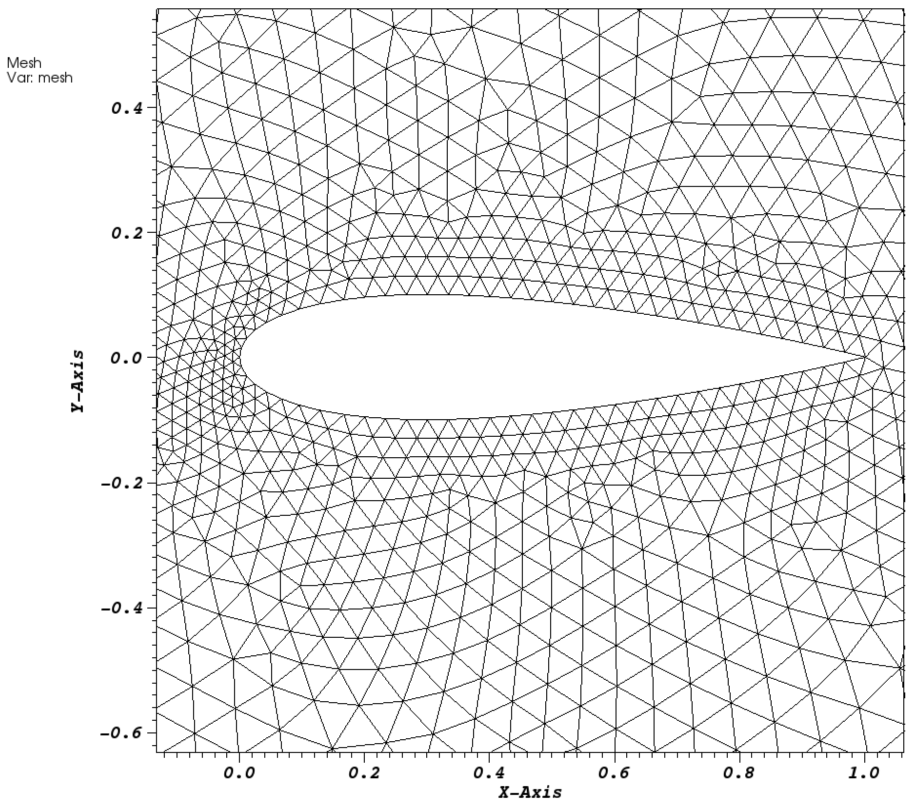


Figure 10: Close Look of Improved Mesh Around Airfoil

Figure 8 , Figure 9 and Figure 10 show mesh of the solution domain. This grids are obtained by using EasyMesh program.Since it is expected that higher velocity gradient at leading edge of the airfoil instead of using coarse mesh at leading at seen in figure 9, more finer mesh distribution and smoother edge is used as seen in figure 10. By doing so, numerical accuracy at the leading edge is highly improved.

### 3.2.2 Angle of Attack 0

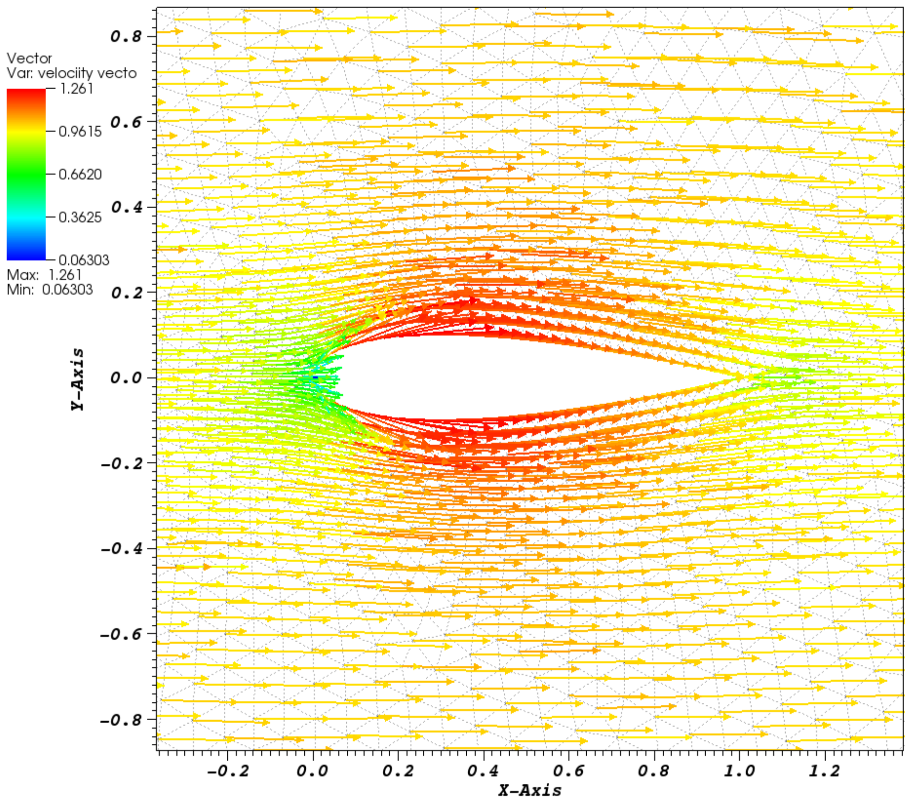


Figure 11: Velocity Vectors Around Airfoil at Angle of Attack 0

In the Figure 11 velocity fields are shown for the angle of attack is equal zero. It is obvious that velocity is zero at the leading edge.Also, velocity increases at the surface of airfoil up to some point due to curvature of the airfoil. Velocity vectors are tangent to that surface as expected. It can be seen that velocity of the fluid, far enough from the solid is getting closer to the free stream velocity.

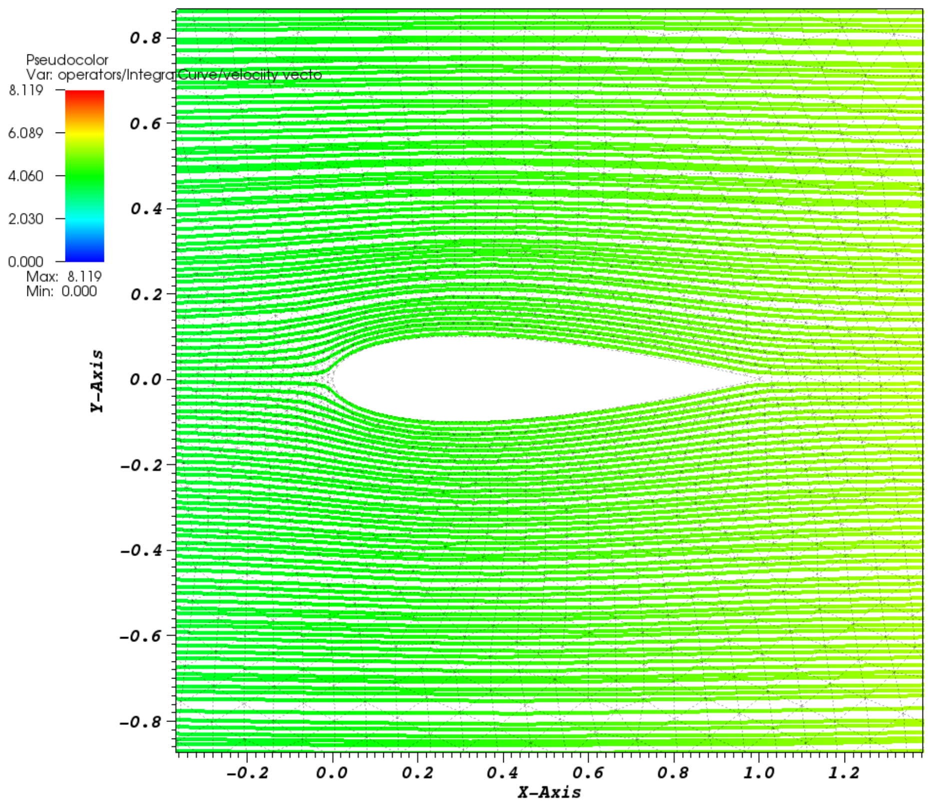


Figure 12: Stream Lines Around Airfoil at Angle of Attack 0

It can be observed from figure 12, the solid surface itself is a streamline and far from the airfoil streamlines gets linear which means does not affected by disturbance of airfoil on flow.

### 3.2.3 Angle of Attack 2

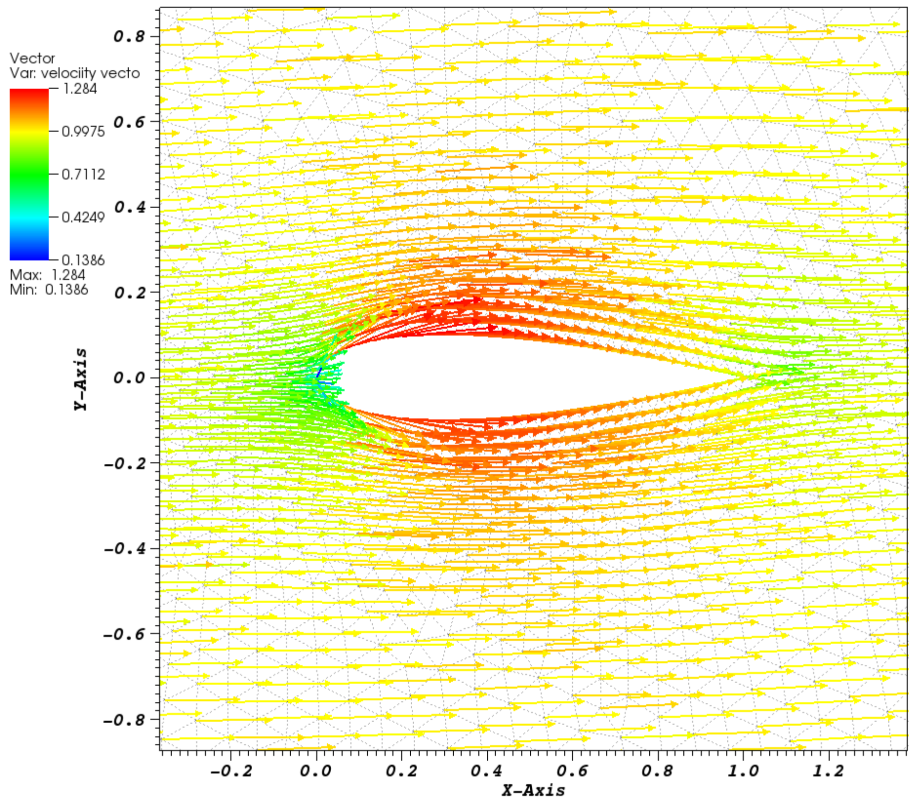


Figure 13: Velocity Vectors Around Airfoil at Angle of Attack 2

It can be seen from figure 13 that at angle of attack 2, stagnation point moves from leading edge to trailing edge by following the airfoil surface from bottom. Also, velocity increases at the surface of airfoil up to some point due to curvature of the airfoil. Velocity vectors are tangent to that surface as expected.

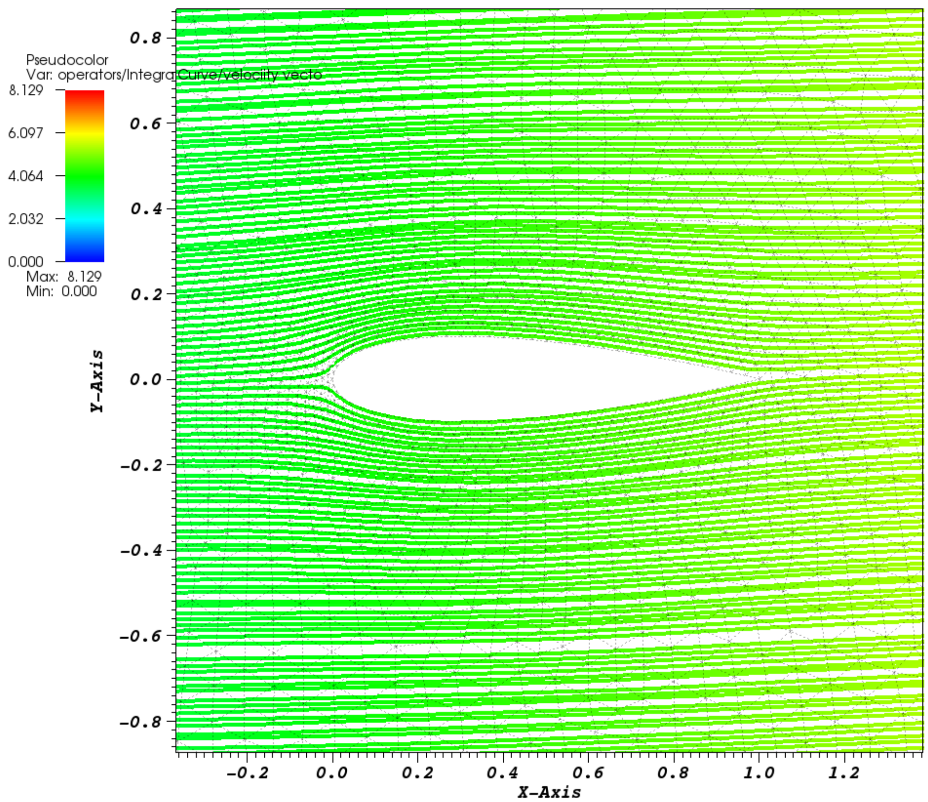


Figure 14: Stream Lines Around Airfoil at Angle of Attack 2

It can be observed from Figure 14, the solid surface itself is a streamline. As angle of attack increase streamlines are getting closer to the direction of free stream velocity.

### 3.2.4 Angle of Attack 5

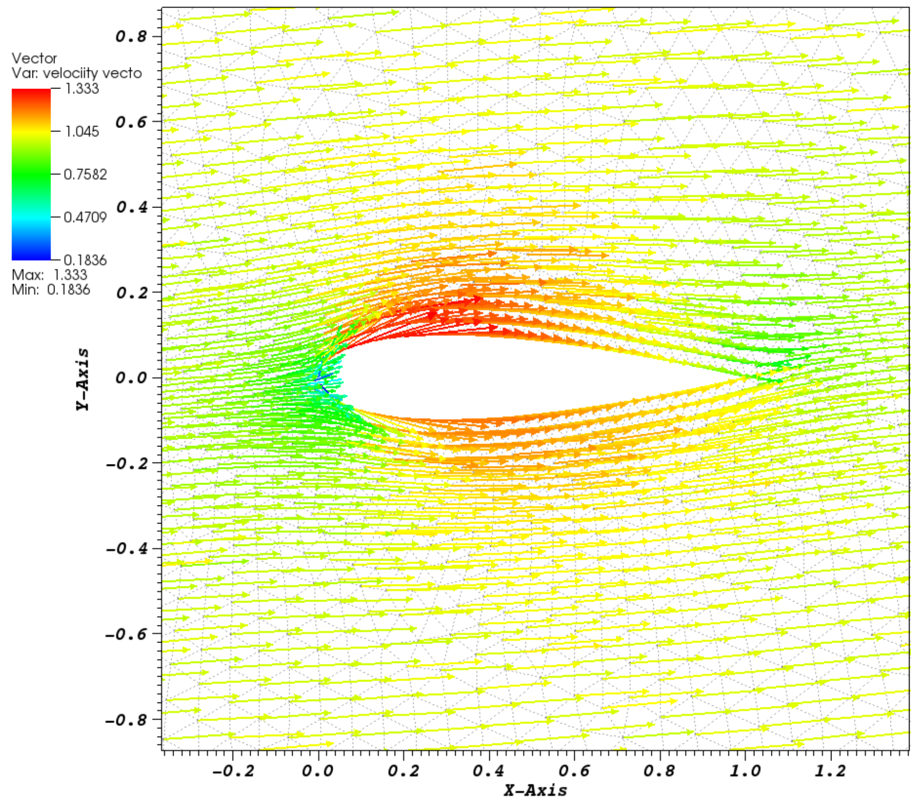


Figure 15: Velocity Vectors Around Airfoil at Angle of Attack 5

It can be seen from Figure 15 that at angle of attack 5, stagnation point moves to trailing edge more than angle of attack 2 case which seen in figure 13.Also, velocity increases at the surface of airfoil up to some point due to curvature of the airfoil. This increase is more than again angle of attack 2 case. Velocity difference between top and bottom are gets much higher, just by observing that it can be expected that lift value of AoA 5 case will be higher than AoA 2 case. It can be seen that velocity of the fluid, far enough from the solid is getting closer to the free stream velocity.

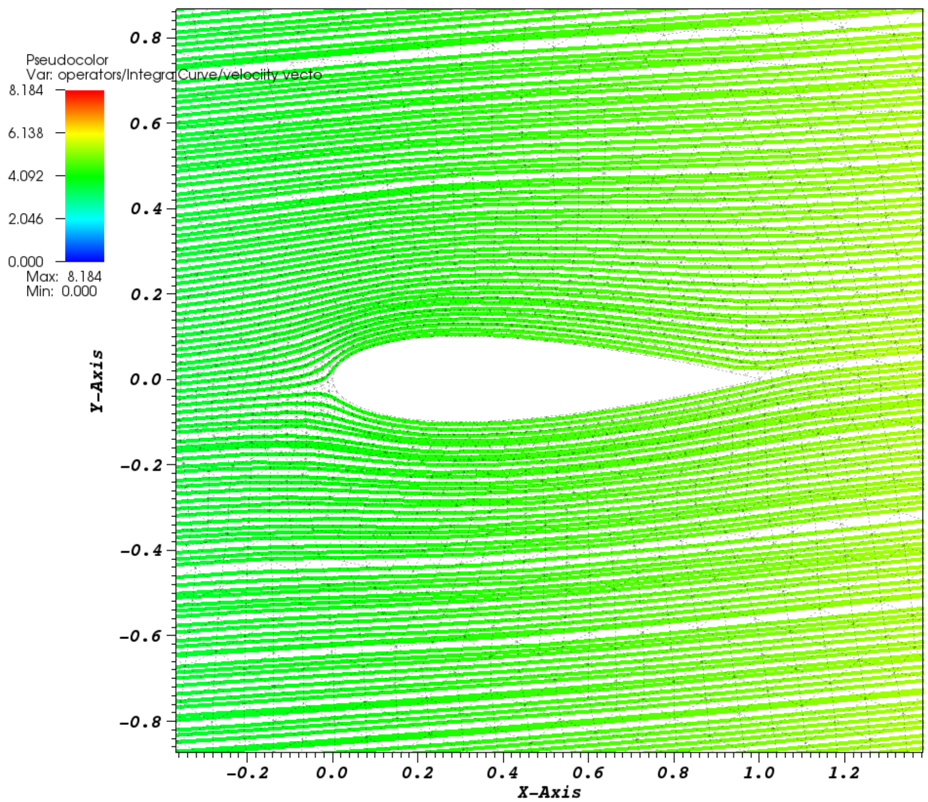


Figure 16: Stream Lines Around Airfoil at Angle of Attack 5

It can be observed from figure 16, the stream lines are smooth and at the trailing edge they come together without any sharp curvature. This means numerical solution might satisfy Kutta condition and have a physical meaning.

### 3.2.5 Angle of Attack 10

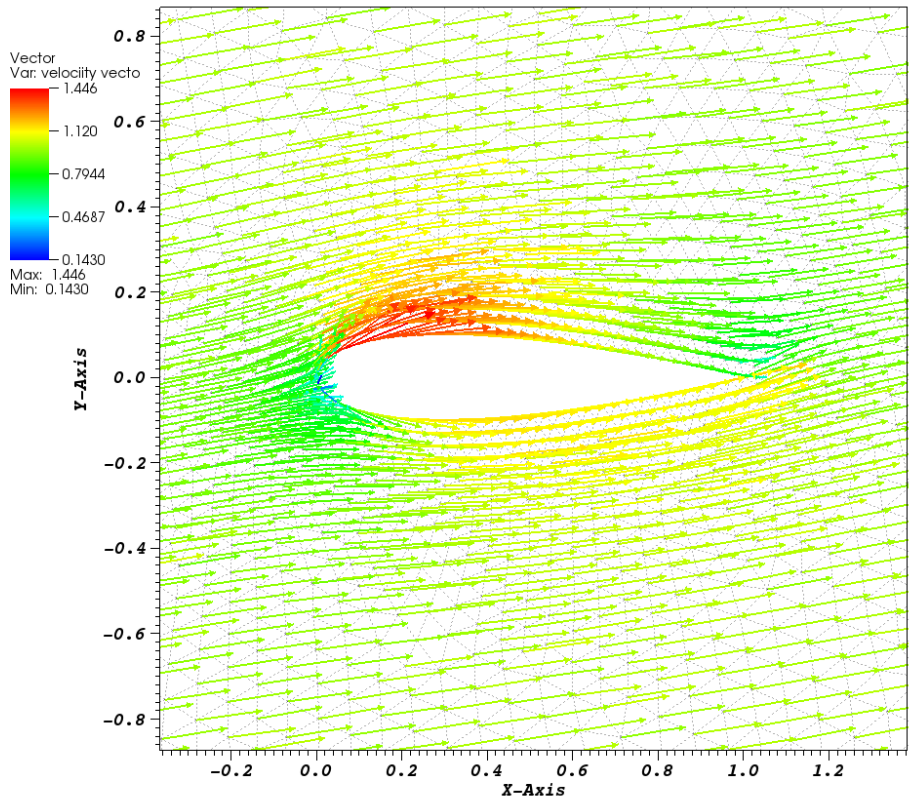


Figure 17: Velocity Vectors Around Airfoil at Angle of Attack 10

It can be seen from figure 17 that at angle of attack 10, goes away from the leading edge of the airfoil.Velocity difference between upper and lower surface becomes obvious. Velocity of upper and lower flow has a great difference at the trailing edge which can be said that Kutta condition is obviously violated and this solution is has no physical meaning in nature even if it is numerically correct.

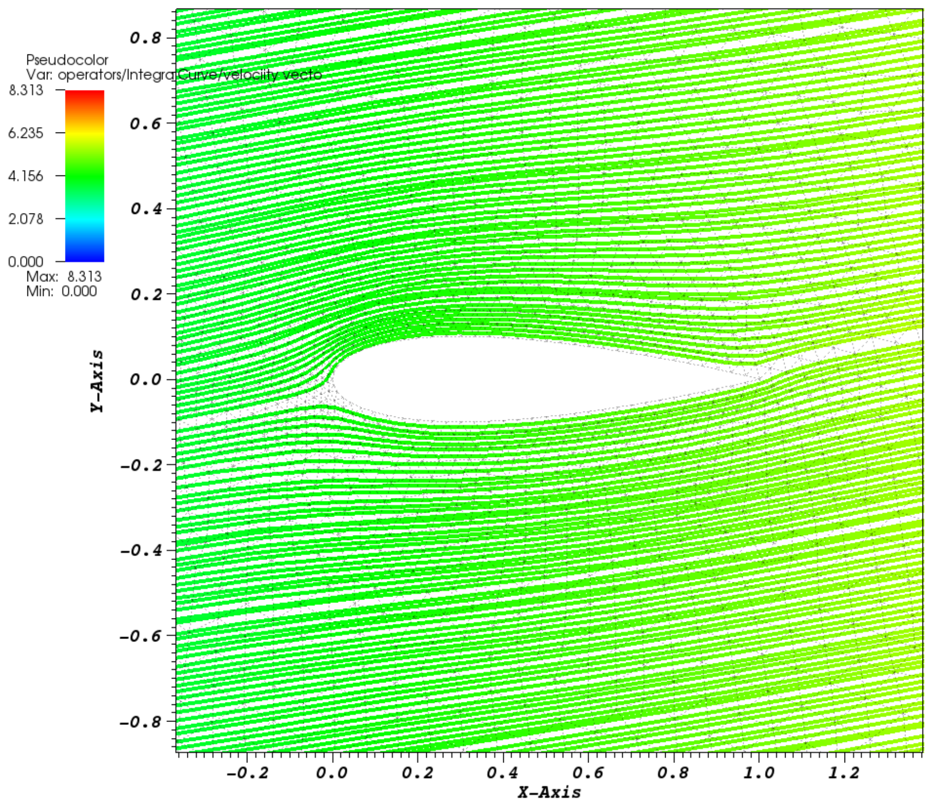


Figure 18: Stream Lines Around Airfoil at Angle of Attack 10

It can be observed from figure 18, streamlines at the trailing edge gets curve to reach each other and some gap occurs occurs between them since a new stagnation point is shown up at the trailing edge. This new stagnation point has a numerical and theoretical meaning but no physical meaning at all.

### 3.2.6 Angle of Attack 20

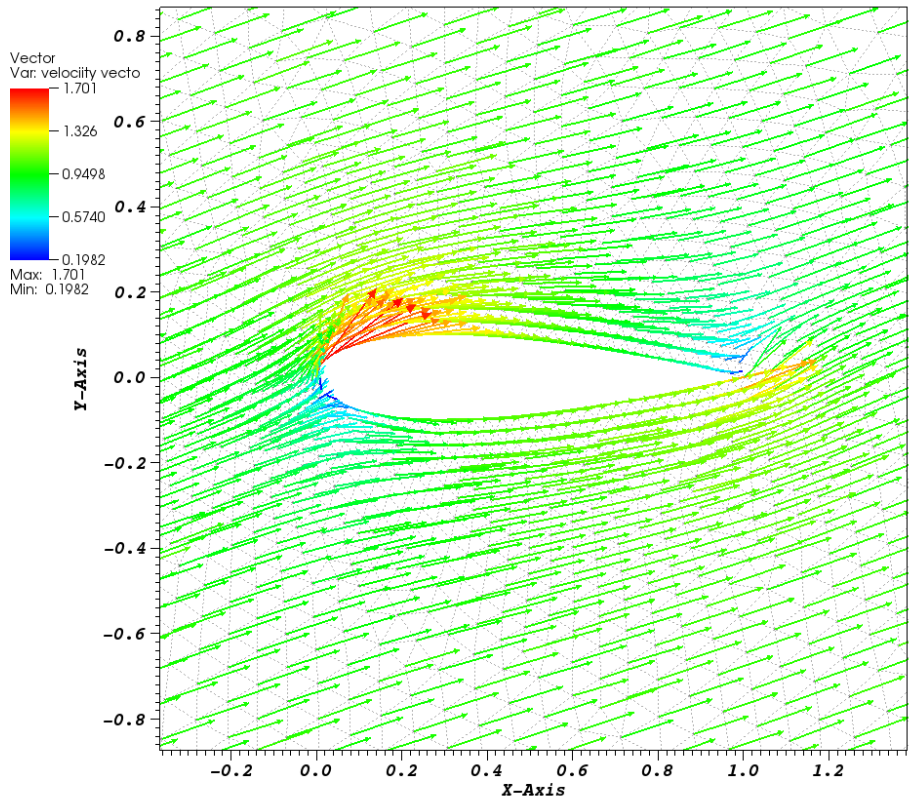


Figure 19: Velocity Vectors Around Airfoil at Angle of Attack 20

To illustrate that leading edge stagnation point and sharp turn at the leading edge phenomena it is chosen that AoA 20. It is more clear in figure 13 there is another stagnation point at the leading edge and velocity gradient at the leading edge so high which causes sharp turns of velocity vectors at the trailing edge. This sign obviously show that this solution is not acceptable for real life applications.

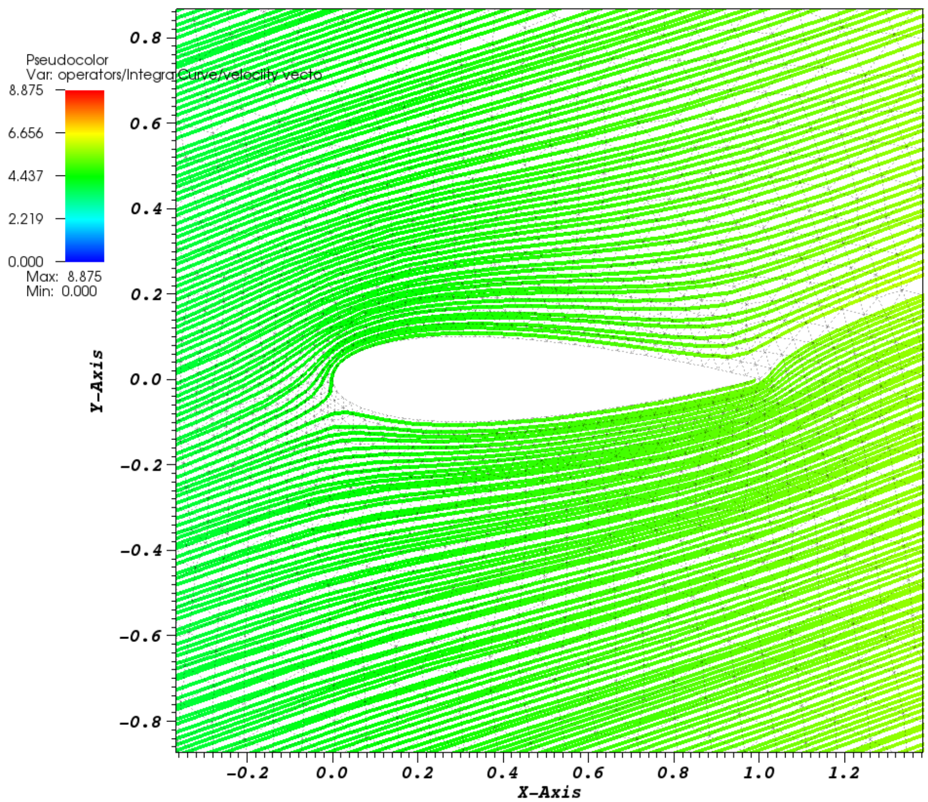


Figure 20: Stream Lines Around Airfoil at Angle of Attack 20

The sharp turn at the trailing edge can be observed in figure 20.

### 3.2.7 $C_p$ distribution on airfoil

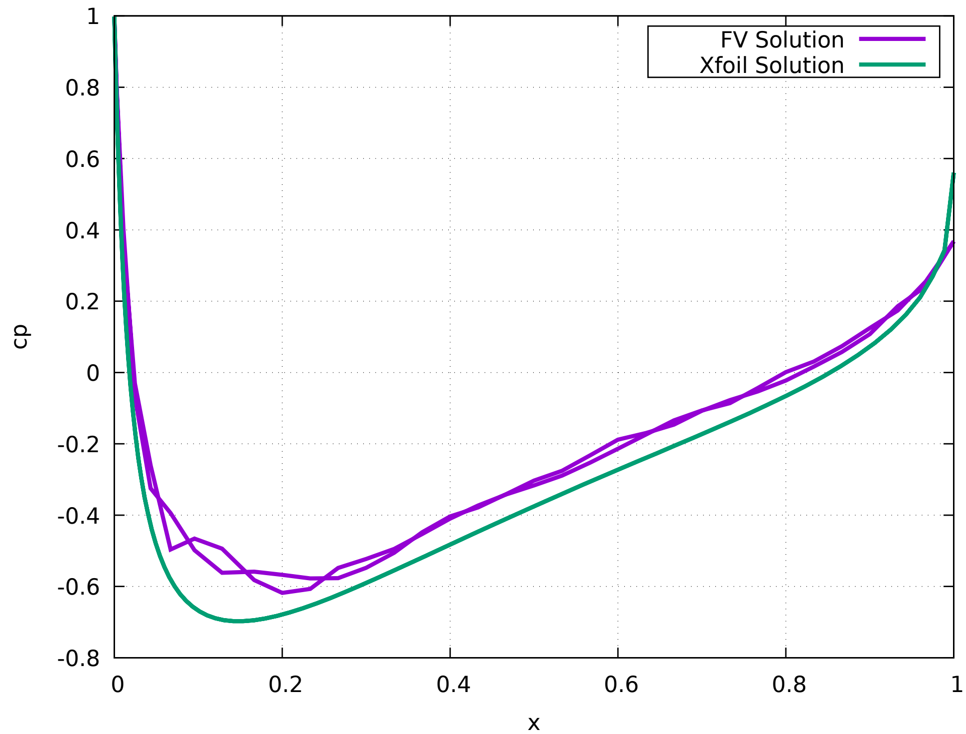


Figure 21: $C_p$ distribution at Angle of Attack 0

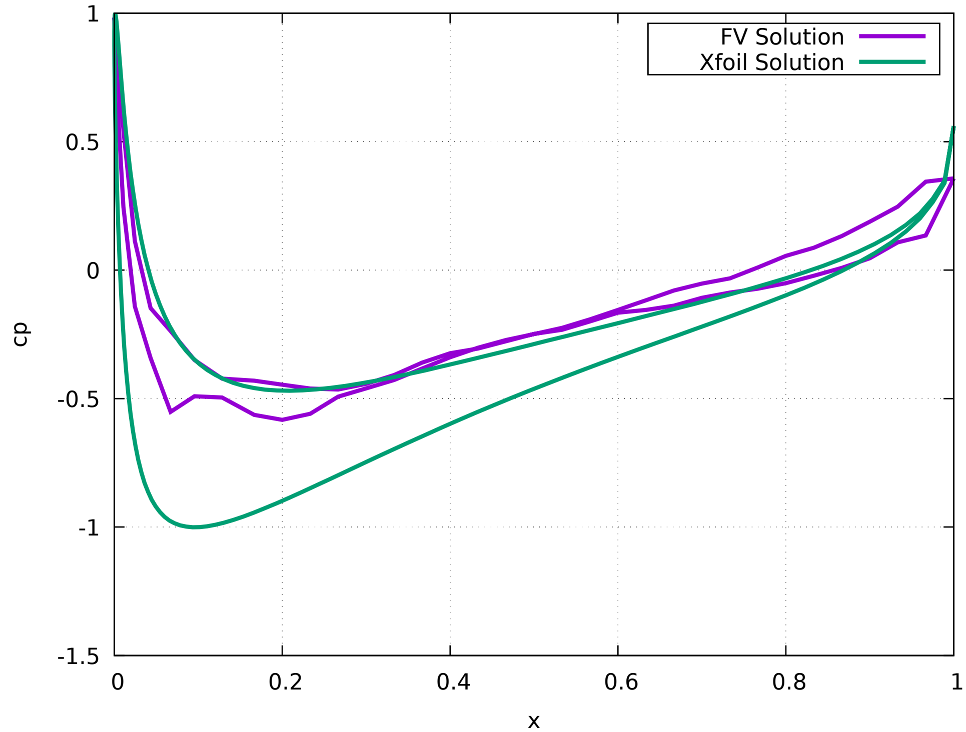


Figure 22: $C_p$ distribution at Angle of Attack 2

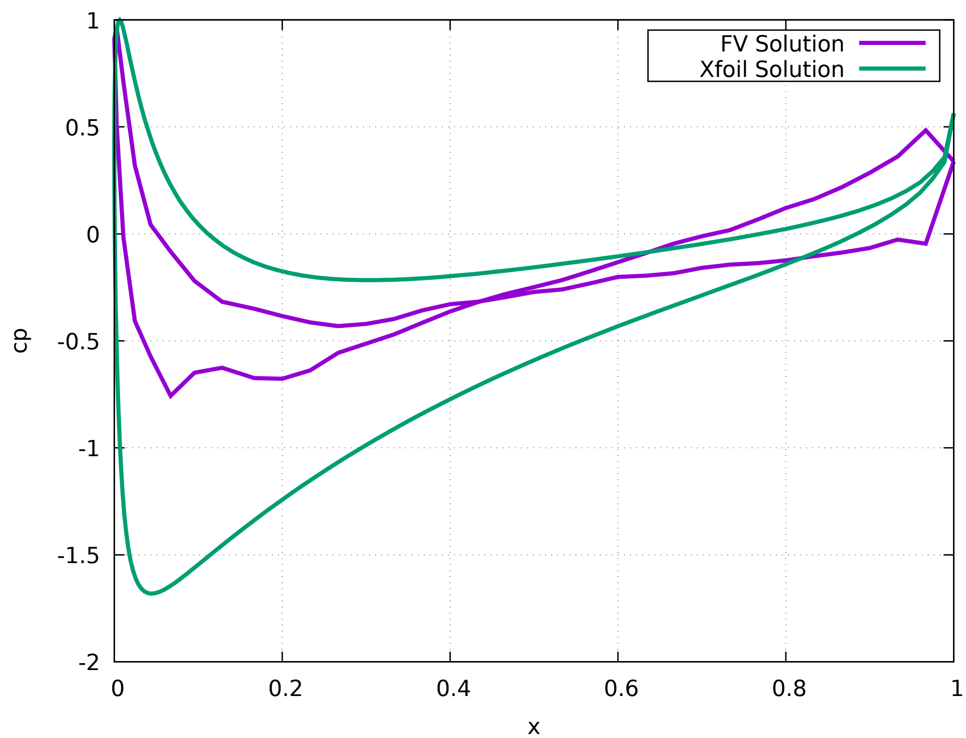


Figure 23: $C_p$ distribution at Angle of Attack 5

It can be seen from Figure 21 , 22 and 23 , $C_p$ distribution of airfoil changes different angle of attack. In the Figure 21, upper and lower $C_p$ values are very close together.This is almost satisfied XFOIL $C_p$ values which is chosen as reference value.The reason of closing $C_p$ values, the airfoil is symmetric airfoil so there must be no difference of upper and lower pressure and lift force doesn't occur at zero angle of attack. As angle of attack increases, FVM and XFOIL $C_p$ distribution difference increase. This difference between FVM and XFOIL $C_p$ distribution is caused by the method difference, as mentioned above FVM calculates values for cells which causes some problems when calculating node values.

#### 3.2.8 Coefficient of $c_d$ and $c_l$ at Different Angle of Attack

In this homework $c_d$ and $c_l$ are computed in three different $\alpha$ values as shown in table below:

| **Angle of Attack** | $c_l$ **FV** | $c_l$ **Xfoil** | $c_d$ **FV** | $c_d$ **Xfoil** |
|---|---|---|---|---|
| 0 | 0 | 0 | 0.02 | 0 |
| 2 | 0 | 0.26 | 0.01 | 0 |
| 5 | 0.02 | 0.64 | 0.01 | 0 |

Table 1: $c_l$ and $c_d$ Values Table

From table 1 it can be said that for calculation of $c_l$ and $c_d$ values using FVM for potential flows is not a good choose.

# 4 Conclusion

In conclusion, velocity fields and streamlines of flow around an cylinder and airfoil are solved by using finite volume method. After that by the help of the Bernoulli equation, velocity is related with pressure. In the circle, velocity increases up to a point where free stream velocity direction is tangent to surface of circle. At the zero angle of attack, stagnation point is seen on the leading edge which is expected from the inviscid flow. In varying angle of attack, stagnation point moves around circle. For example, while angle of attack increases, stagnation point moves to below of the circle with same angle. Stagnation point occurs points where the free stream velocity direction is perpendicular to the surface. Although the angle of attack changes, velocities and streamlines on the surface are symmetric with respect to the direction of free stream. The reason is coming from the symmetry of the circular cylinder.
In the airfoil, velocity increase up to some point again as it follows the airfoil surface from above and below the leading edge. At zero angle of attack stagnation point is seen at the leading edge as expected. At that point velocity is zero. Also at that angle, velocity field and stream lines are symmetric with respect to the chord line of airfoil. The reason is due to having non-cambered airfoil. Also because of this symmetry in airfoil there is no same velocity distribution at lower and upper surface at AoA 0. Therefore, lift force is not created. In varying angle of attack on airfoil, stagnation point moves from leading edge to trailing edge as $\alpha$ increases. Velocity field and streamlines are not symmetric with respect to free stream direction because airfoil itself is not symmetric according to free steam velocity direction. Also, it is observed that for higher angles of attacks solution has no physical meaning but they are numerically correct. FVM is not a acceptable method for calculation of force coefficient for potential flows however it has great capability of visualizing flow around object.